

# The NHL-domain protein Wech is crucial for the integrin–cytoskeleton link

Birgit Löer<sup>1</sup>, Reinhard Bauer<sup>1</sup>, Roland Bornheim<sup>2</sup>, Jessica Grell<sup>2</sup>, Elisabeth Kremmer<sup>3</sup>, Waldemar Kolanus<sup>2</sup> and Michael Hoch<sup>1,4</sup>

Integrin transmembrane receptors mediate cell adhesion through intracellular linker proteins that connect to the cytoskeleton<sup>1,2</sup>. Of the numerous linker proteins identified, only a few, including Talin and Integrin-linked-kinase (ILK), are essential and evolutionarily conserved. The *wech* gene encodes a newly discovered and highly conserved regulator of integrin-mediated adhesion in *Drosophila melanogaster*. Embryos deficient in *wech* have very similar phenotypes to *integrin*-null or *Talin*-null embryos, including muscle detachment from the body wall. The Wech protein contains a B-box zinc-finger and a coiled-coil domain, which is also found in RBCC/TRIM family<sup>3</sup> members, and an NHL domain<sup>4</sup>. In  $\beta$ -integrin or Talin mutants, Wech is mislocalized, whereas ILK localization depends on Wech. We provide evidence that Wech interacts with the head domain of Talin and the kinase domain of ILK, and propose that Wech is required to connect both core proteins of the linker complex during embryonic muscle attachment. Both the NHL and the B-box/coiled-coil domains of Wech are required for proper interaction with Talin and ILK. The single murine Wech orthologue is also colocalized with Talin and ILK in muscle tissue. We propose that Wech proteins are crucial and evolutionarily conserved regulators of the integrin–cytoskeleton link.

The formation of complex tissues in animals often involves stable adhesion between different cell layers and extracellular matrix substrates, which is, to a large extent, mediated by members of the integrin family of heterodimeric transmembrane receptors<sup>1,2,5–8</sup>. Loss of integrins causes muscle detachment in flies and mice<sup>6,7</sup>. Integrin mutations or aberrant expression can result in skin diseases, such as epidermolysis bullosa, and contribute to invasion and metastasis during cancerogenesis<sup>9</sup>. A crucial part of the adhesive function of integrins is their ability to connect to the actin cytoskeleton. This involves a complex of adaptor proteins, which bind to the cytoplasmic tail of integrins and mediate the link to the cytoskeleton. Although many proteins have been identified that may

contribute to the linker complex<sup>10,11</sup>, in mammals, flies and worms only a few components have been identified as essential to the link. These include Talin<sup>12</sup>, ILK<sup>13</sup>, PINCH<sup>14</sup> and Tensin<sup>15</sup>, encoding an actin-capping protein, which coordinates signalling with cytoskeletal changes. Recent studies in mammalian cells and in *Drosophila* suggest that Talin is necessary for the initial formation of the integrin adhesion complex<sup>16,17</sup> and reinforces it, possibly by recruiting other proteins, including ILK and Tensin<sup>15,18</sup>. Absence of Talin causes defects that are almost identical to those seen in the absence of integrin, such as muscle detachment and failure of germ-band retraction during embryonic development. In contrast, absence of other components of the link causes only a subset of the defects. In different types of cells, integrins make diverse connections with the actin cytoskeleton; however, the molecular basis for the cell-type specific functions of integrins is still mostly unknown.

In a search for genes controlling integrin-mediated muscle attachment in *Drosophila* embryos, we identified two P insertions and generated one imprecise excision allele — that we named *wech* — affecting a previously uncharacterized genetic locus (Supplementary Information, Fig. S1). In homozygous embryos of the imprecise excision allele, *wech*<sup>66</sup>, *wech* transcript and protein levels were markedly reduced when compared with wild-type embryos. In *wech*<sup>66</sup> germline clone embryos, Wech protein levels were reduced substantially and were barely detectable (Supplementary Information, Figs S1, S2), indicating that *wech*<sup>66</sup> is an amorphic allele. Molecular analysis, reversion of the phenotype by perfect excision of the P elements and genetic rescue experiments demonstrate that the lethality of *wech* alleles is linked to *wech* gene function (see Methods; Supplementary Information, Fig. S1).

Phenotypic analysis of homozygous *wech*<sup>66</sup> mutants and of trans-heterozygous combinations with a deficiency (see Methods) indicates an essential role of *wech* in muscle attachment during *Drosophila* embryogenesis (*wech* is a German Rhineland term for ‘detached’ or ‘gone’). During embryonic development, the somatic muscles attach to each other and to their anchoring points in the epidermis, the tendon cells, to generate a highly stereotyped pattern of 30 muscles in each abdominal

<sup>1</sup>Life and Medical Sciences Institute (LIMES), Program Unit Development & Genetics, Laboratory for Molecular Developmental Biology, University of Bonn, Meckenheimer Allee 169, D-53115 Bonn, Germany. <sup>2</sup>LIMES-Institute, Program Unit Molecular Cell and Immune Biology, Laboratory for Molecular Immunology, University of Bonn, Karlrobert-Kreien-Str.13, D-53115 Bonn, Germany. <sup>3</sup>Helmholtz Zentrum München, Institut für Molekulare Immunologie, Marchioninistr. 25, 81377 München, Germany.

<sup>4</sup>Correspondence should be addressed to M.H. (e-mail: m.hoch@uni-bonn.de)

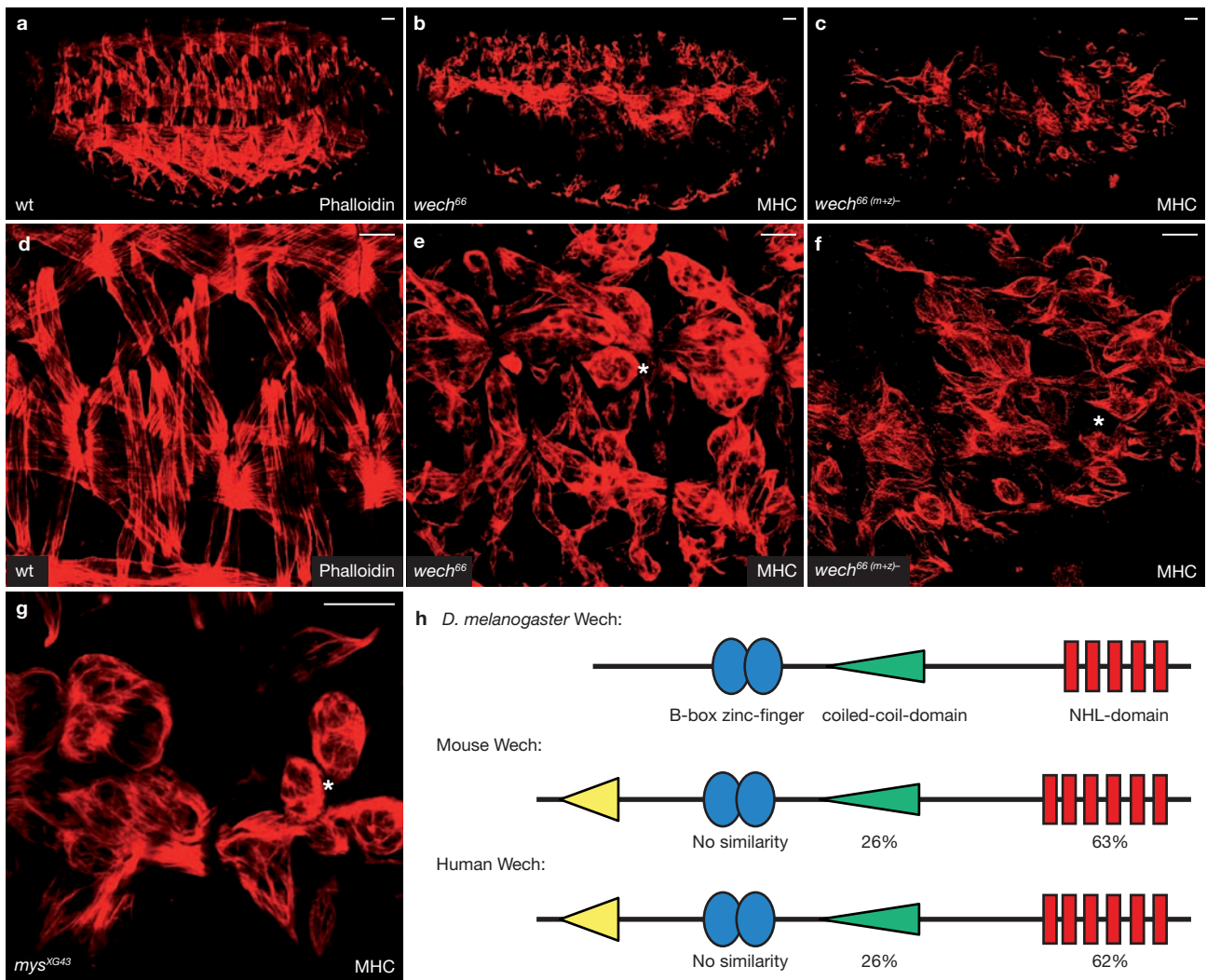


**Figure 1** Characterization of the *wech* mutant phenotype. (a–f) Muscle staining in late-stage-16/early-stage-17 mutant embryos. *wech*<sup>66</sup> zygotic mutants (b, detail in e) show rounded-up and detached muscles compared with wild-type (wt in a, detail in d). Enhancement of the mutant phenotype in stage 15/16 *wech*<sup>66</sup> maternal and zygotic mutants (c, detail in f). (g) The *wech*<sup>66</sup>

muscle-detachment phenotype is similar to that of *mys* mutant embryos. (e–g) Multinucleated and detached muscles are marked with an asterisk. (h) Predicted domain structure of *Drosophila* Wech, compared with mouse and human Wech. Indicated are the amino-acid sequence identities (%) among the different domains. Scale bars are 20  $\mu\text{m}$  (a–c) and 10  $\mu\text{m}$  (d–g).

hemi-segment<sup>19,20</sup> (Fig. 1a, d). The cytoskeletal network forms bridges between the muscle and the tendon cell through dense hemi-adherens-type junctions formed between the tendon cell, the muscle and a thick layer of extracellular matrix material that is deposited in the space between them<sup>19</sup>. This architecture provides the mechanical force that is required to resist muscle contraction during larval locomotion. The muscles start to attach to the tendon cells at embryonic stage 15 and during the last two stages of embryogenesis (stages 16 and 17) the attachment of the muscles to the tendon cells is elaborated by expansion of the hemi-adherens junctions, accumulation of tendon matrix and increased expression of  $\beta$ 1-tubulin<sup>14,20,21</sup>.

In late-stage embryos homozygous for *wech*<sup>66</sup>, we found that muscles were detached from the body wall (Fig. 1b, e). This mutant phenotype became apparent at embryonic stage 16 and was enhanced during subsequent development, as the force of muscle contraction had increased (Fig. 1). Myosin heavy chain (MHC) staining of stage 17 mutant embryos showed defects in most of the muscles at that point in

development. When both the maternal and zygotic contributions of *wech* were removed (Fig. 1c, f), the detachment phenotype was more severe and became apparent at stage 15, indicating that *wech* has a maternal contribution, which is consistent with its ubiquitous expression during early stages of embryogenesis (Supplementary Fig. S2). Most of the muscles were multinucleated, indicating that *wech* mutants show no major defect in myoblast fusion (Supplementary Information, Fig. S2). Analysis of DA1 (dorsal acute muscle 1) development in *wech* mutants further indicates that muscle differentiation and myoblast fusion are not affected<sup>22</sup>. Rather, the data suggest a role of *wech* in muscle attachment, consistent with the late manifestation of the muscle detachment phenotype. Mutants for  $\beta$ PS integrin (Fig. 1g) or Talin show phenotypes remarkably similar to *wech* mutants<sup>12,23,24</sup>.

The *wech* gene encodes a multidomain protein containing a B-box zinc-finger domain and a coiled-coil domain characteristic of the RBCC/TRIM protein family<sup>3</sup> (Fig. 1h). Members of this family usually contain a tripartite motif composed of a RING domain, one or two B-box motifs

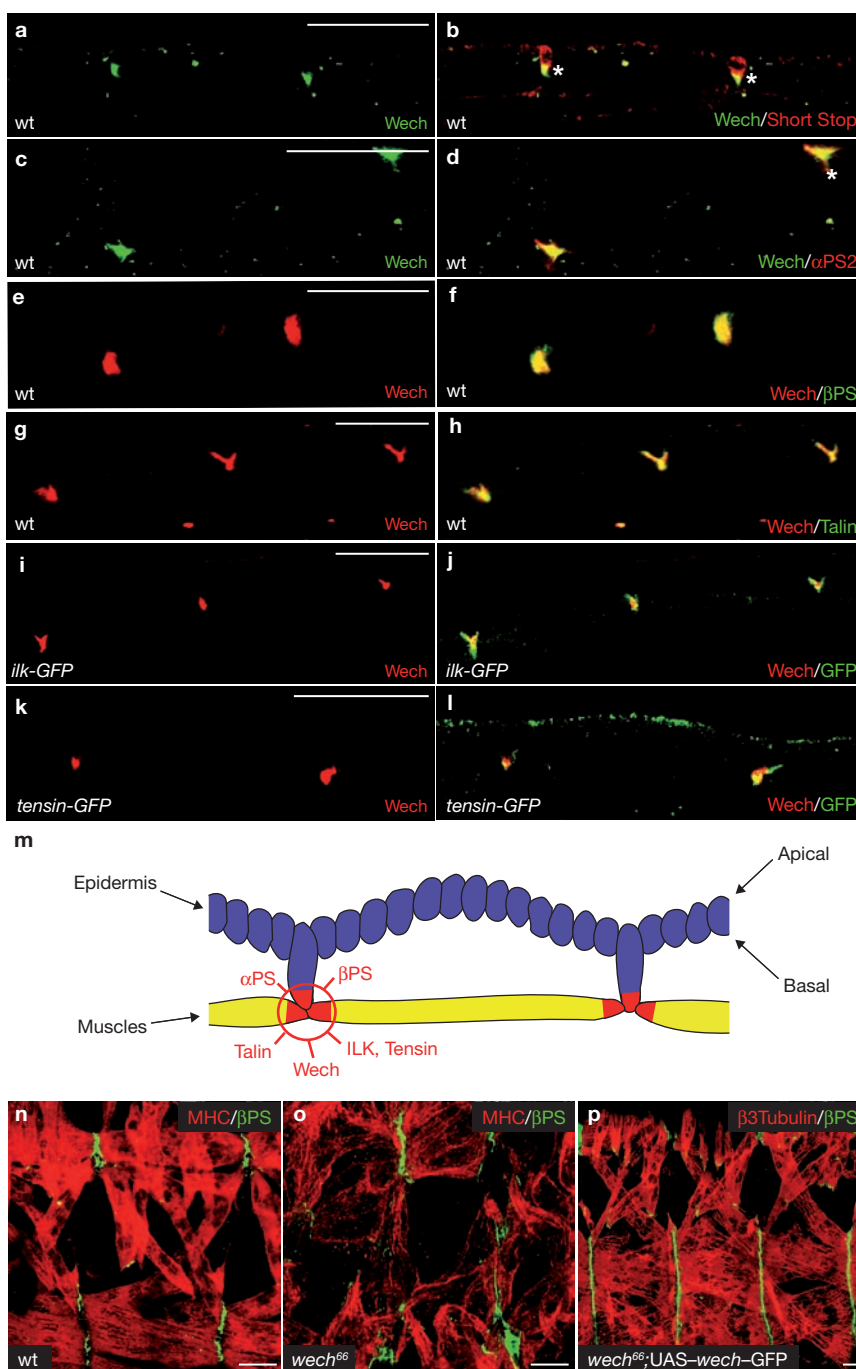


**Figure 2** Wech localization in the epidermal muscle attachment site. (a–l) Wech protein expression in the epidermal muscle attachment site. Wech colocalized with Short Stop (a, b),  $\alpha$ PS2 integrin (c, d),  $\beta$ PS integrin (e, f) and also with the components of the cytoplasmic integrin linker complex, including Talin

(g, h), ILK (i, j) and Tensin (k, l). (m) Summary of the localization data in the attachment site. (n–p) The muscle-detachment phenotype of *wech* mutants (o, compared with wt in n) could be rescued by expression of UAS-*wech*-GFP in both the tendon cells and in the muscles (p). Scale bars are 10  $\mu$ m.

and a coiled-coil region. The *Drosophila* Wech protein does not contain a RING domain; however, it contains a carboxy-terminal NHL domain<sup>4</sup>, which is also found in the *Drosophila* tumour suppressor proteins Brat<sup>25</sup> and Mei-P26 (ref. 26). In addition to Wech, *brat* and *mei-P26* encode the only two other NHL-domain-containing family members in *Drosophila*. Molecular characterization of hypomorphic mutations in the *brat* gene suggests that the NHL domain carries the tumour suppressor function of this protein<sup>25</sup>. Single-copy genes of *wech* orthologues are found in

other invertebrates and in mammals, including mice, rats and humans (Fig. 1h). The *Caenorhabditis elegans* Wech orthologue is named Lin-41 and is involved in the regulation of the progression from larval (L) stage 4 to the adult developmental programme<sup>27</sup>.

To study the molecular function of Wech, we generated an anti-Wech antibody (see Methods; Supplementary Information, Fig. S1). Immunostaining indicates that Wech protein is expressed ubiquitously in all epithelial cells during early stages of embryogenesis (Supplementary

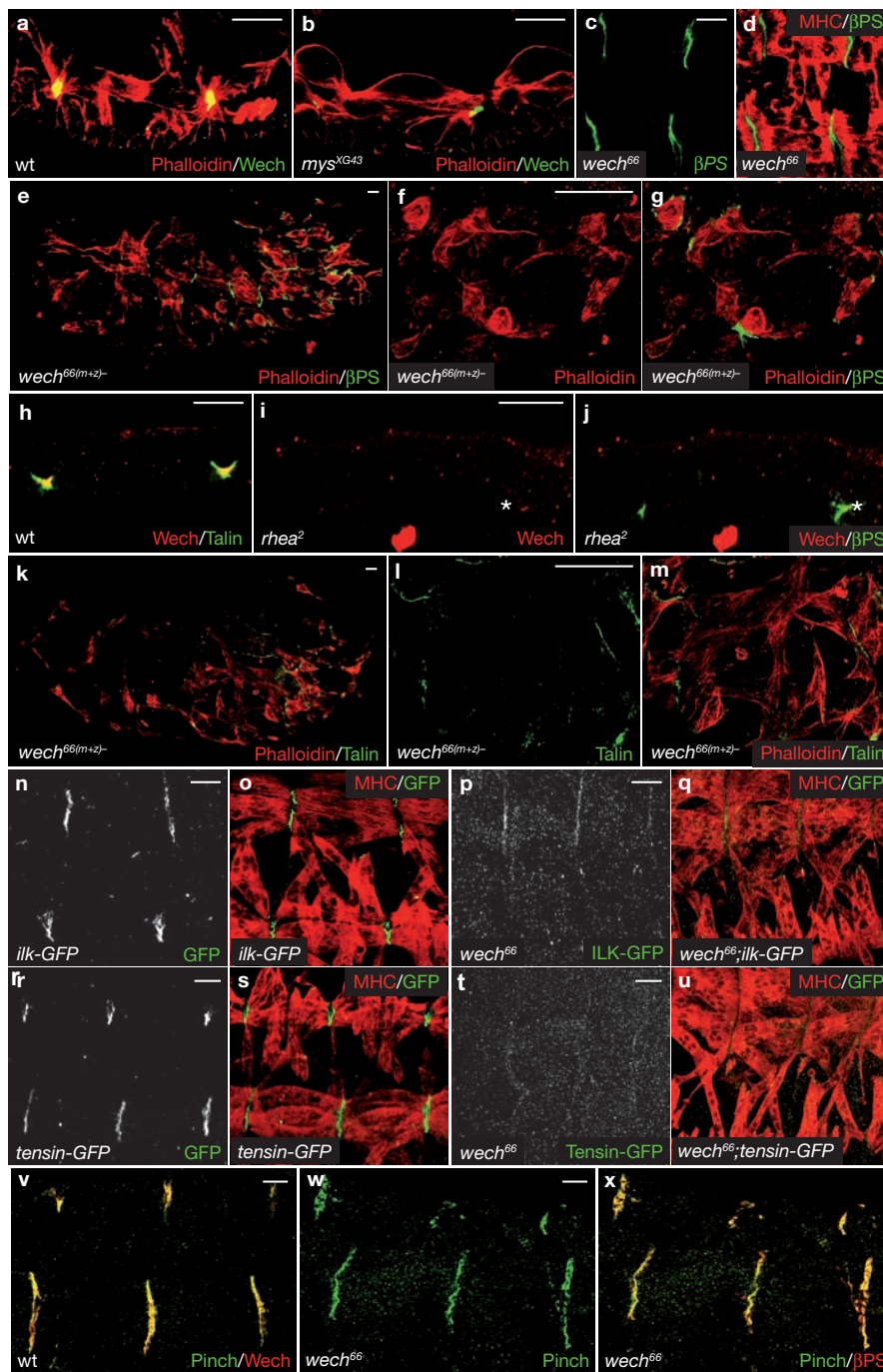


**Figure 3** Wech function in the muscle attachment sites. (a–x) Late-stage-16 embryos. When compared with wt embryos (a), Wech was markedly reduced and mislocalized in late-stage-16 zygotic *mys* mutants (b). (c–g)  $\beta$ PS integrin localization was not altered in zygotic *wech*<sup>66</sup> mutants (c, d) or maternal and zygotic *wech*<sup>66</sup> mutants (e–g). (h–m) Wech failed to localize in Talin (*rhea*<sup>2</sup>) mutants (asterisk in i and j), compared with wt (h). However, Talin was still

expressed in the attachment site in *wech*<sup>66</sup> maternal and zygotic mutants (k–m). (n–u) Both ILK (p, q) and Tensin (t, u) were markedly reduced in *wech*<sup>66</sup> mutants as compared with wt in (n, o) and (r, s), respectively. Note that MHC co-staining serves as an internal control. (v–x) PINCH expression was not altered in zygotic *wech* mutants (w, x), compared with wt (v). Scale bars are 10  $\mu$ m for all except e, k (20  $\mu$ m).

Information, Fig. S2). After germ-band retraction, Wech accumulated specifically in the muscle attachment sites (Fig. 2a–m and Supplementary Information, Fig. S2). Co-immunostaining with the tendon and muscle-cell markers Short Stop and  $\alpha$ PS2, respectively, indicate that Wech is highly localized in both cell types in a cortical localization at the attachment site (Fig. 2a–d).  $\beta$ PS Integrin (Fig. 2e, f) and components of the

cytoplasmic integrin-linked complex, Talin, ILK and Tensin, which bind to the cytoplasmic tail of  $\beta$ PS integrin, colocalized with Wech (Fig. 2g–l; schematic representation in Fig. 2m). Consistent with the expression of Wech in both the tendon and the muscle cells, the muscle detachment defect was rescued when Wech was re-supplied in both the tendon and muscle cells, using a combination of *sr-GAL4* (tendon-cell-specific) and

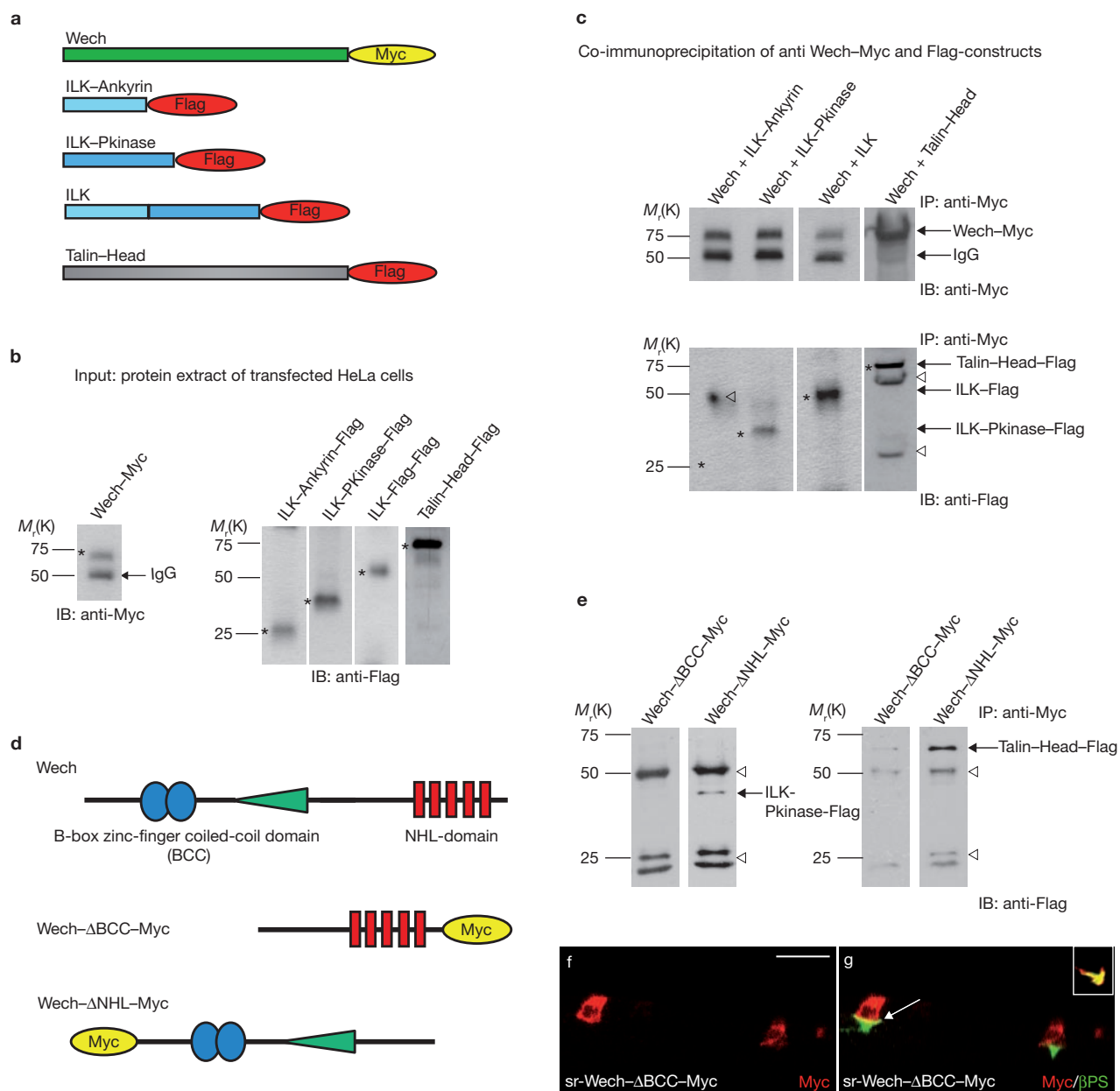


**Figure 4** Wech interacts with Talin and ILK. **(a)** Schematic representation of tagged fusion proteins of Wech, ILK and Talin. **(b)** Expression of co-transfected Myc-tagged Wech with either Flag-tagged ILK-Ankyrin, ILK-protein kinase domain (ILK-Pkinase), ILK or Talin-head domains in HeLa cells, verified by immunoprecipitation (IP) and immunoblot (IB). Bands corresponding to the size of the tagged fusion proteins are depicted by an asterisk. **(c)** Co-immunoprecipitation of Wech-Myc with each of the Flag-tagged constructs. The IP of Wech-Myc was confirmed by western blotting using an anti-Myc antibody (upper panel). The interaction of Wech-Myc with Flag-tagged constructs was analysed by western blotting using an anti-Flag antibody (lower panel). Wech interacted with the protein kinase domain, but not with the ankyrin-repeat domain of ILK. Wech also interacted with the head-domain of Talin. Non-specific bands are marked with an arrowhead, specific bands are marked with an asterisk

*mef-GAL4* (muscle-cell-specific) in combination with UAS-*wech*-GFP (Fig. 2n-p and Methods). Whereas *wech*<sup>66</sup> mutants are embryonic lethal, the rescued animals survived until the third instar-larval stage. Similarly, rescue could be obtained when Wech was ubiquitously expressed using

**(d)** Wech deletion constructs. **(e)** Co-immunoprecipitation of Wech deletion variants with ILK-Pkinase and Talin-head domains. The ILK-Pkinase domain interacted with the Wech-BCC domain (Wech-ΔNHL), but not with the NHL domain (Wech-ΔBCC). In contrast, the Talin-head domain interacted with both the BCC domain (Wech-ΔNHL) and the NHL domains. Bands corresponding to the tagged fusion proteins are depicted by an arrow. Non-specific bands are marked with an arrowhead. **(f, g)** Transgenic embryos expressing a UAS-Myc-tagged Wech-ΔBCC construct in tendon cells using the *sr-GAL4* driver. Although the protein fragment accumulated in the cytoplasm, colocalization with βPS integrin in the attachment site still occurred (arrow in g). Inset in (g) shows overexpression of Wech in the tendon cell and colocalization with βPS integrin. Scale bar is 10 μm. Full scans and panels of key western blot data are shown in Supplementary Information, Fig. S5.

*hs-GAL4::UAS-wech*-GFP or when the single driver lines, *sr-GAL4* or *mef-GAL4* were used, indicating that Wech expression rescues in either cell type (see Methods). The latter finding is surprising and may be due to the residual maternal component in the muscles.

To test whether Wech is involved in integrin-mediated cell adhesion, we first analysed the expression of Wech in  $\beta$ PS integrin (*mysospheroïd*, *mys*) mutants. In zygotic *mys* mutants, the highly localized cortical accumulation of Wech at the attachment site failed and protein was also found in other parts of the cytoplasm at reduced levels (Fig. 3a, b). Consistently, a failure of cortical Wech localization was also found in zygotic and maternal *mys* mutants (Supplementary Information, Fig. S2). These data indicate that  $\beta$ PS integrin is required for Wech localization. In contrast,  $\beta$ PS integrin was still properly localized in zygotic *wech*<sup>66</sup> mutants (Fig. 3c, d) and in maternal and zygotic *wech* germline clone embryos, in which Wech protein expression was markedly reduced (Fig. 3e–g; Supplementary Information, Fig. S2). As Talin is known to interact through its head domain with integrin cytoplasmic tails<sup>12,18</sup>, we analysed Wech localization in amorphic Talin (*rhea*<sup>2</sup>) mutants. In *rhea* mutants, Wech localization was markedly reduced (Fig. 3h–j), whereas in maternal and zygotic *wech* mutants, Talin seemed to be unchanged (Fig. 3k–m). This indicates that Talin is required for Wech localization. In contrast, Wech was required for proper ILK localization. In *wech* mutants, ILK localization at the attachment site was reduced (compare Fig. 3n, o with p, q), whereas Wech was still localized properly in *ilk* mutants (Supplementary Information, Fig. S3). Consistent with these data, Tensin, which is known to require ILK for its localization<sup>15</sup>, failed to accumulate at the attachment site in *wech* mutants (compare Fig. 3r, s with t, u). PINCH, which was shown to modulate ILK function by direct binding or by recruitment of an ILK-modifying factor<sup>14</sup>, was still localized properly in *wech* mutants (Fig. 3v–x). In contrast to *wech* mutants, ILK was still concentrated at the muscle attachment sites in PINCH (*steamer duck*) mutant embryos<sup>14</sup>. This suggests that Wech may be required to link an ILK-containing multiprotein complex to Talin, and PINCH may function as a molecular scaffold supporting the assembly of the ILK-containing linker multiprotein complex. Our finding that the *wech* mutant phenotype is similar in severity to *talin* mutants and stronger than that of *ilk* mutants, suggests that other unknown factors, in addition to ILK, may depend on Wech function during muscle attachment.

To further analyse the putative role of Wech in integrin-mediated adhesion, we performed biochemical co-immunoprecipitation analysis. We used extracts of mammalian HeLa cells expressing tagged fusion proteins of the *Drosophila* Wech, Talin, ILK or various subdomains of these proteins (Fig. 4a). We found that Wech interacts with the protein kinase domain but not with the ankyrin-repeat domain of ILK (Fig. 4b, c). Furthermore, Wech interacts with the head domain of Talin (Fig. 4c). Co-immunoprecipitation analysis using *Drosophila* embryonic extracts further confirmed the interactions of Wech with Talin (Supplementary Information, Fig. S3) and ILK (data not shown). To determine which protein domains of Wech may be required for its interaction with Talin and ILK at the muscle attachment sites, we generated Myc-tagged Wech protein variants with deletions of the N-terminal B-box zinc-finger and coiled-coil domains (Wech- $\Delta$ BCC) or the C-terminal NHL domain (Wech- $\Delta$ NHL; Fig. 4d; Supplementary Information, Fig. S3). The deletion constructs were expressed in HeLa cells (Fig. 4e) or in transgenic embryos (Fig. 4f, g) and tested for interaction with ILK and Talin. In co-immunoprecipitation experiments using HeLa-cell extracts, we found that the BCC domain of Wech is essential for binding to the protein kinase domain of ILK (Fig. 4e, left panel), whereas the head domain of Talin interacted with both the BCC and the NHL domains of Wech (Fig. 4e, right panel). *In vitro*, the interaction of the Talin head domain with the Wech BCC domain was, however, much stronger

when compared with its interaction with the Wech NHL domain (Fig. 4e; Methods). When expressing the Wech protein deletion variants as Myc-tagged versions in the tendon cells using the strong *sr-GAL4* driver, both deletion variants accumulated mainly in the cytoplasm, and colocalization with  $\beta$ PS Integrin, Talin or ILK was markedly reduced (Fig. 4f, g and data not shown). This suggests that both the BCC and NHL domains of Wech may be required *in vivo* for its proper localization at the muscle attachment sites.

As mentioned above, single-copy genes of *wech* orthologues are found in flies, worms and mammals, including mice and humans (Fig. 1h). To investigate whether the murine Wech orthologue may be involved in integrin-mediated processes, we generated an antibody against the protein and studied its expression in adult mice (Supplementary Information, Fig. S4). We found that the murine Wech protein was expressed in the sarcomeric Z-discs of adult muscles where it was colocalized with ILK (Supplementary Information, Fig. S4), which has been identified recently as an architectural component of the Z-disc of heart muscles in zebrafish<sup>28</sup>. Strong colocalization of murine Wech was also found with costameric Talin (Supplementary Information, Fig. S4). Notably, only partial colocalization was detected with sarcolemmal  $\beta$ 1 integrins (Supplementary Information, Fig. S4). These results are consistent with the notion that Wech serves as a conserved adaptor, which is required for linking Talin and ILK in the integrin multiprotein complex.

In summary, we show that Wech is a crucial component for the physical link between integrins and the cytoskeleton in the *Drosophila* epidermal muscle attachment sites. We propose that Wech connects integrins and the cytoskeleton in the attachment sites by interacting with Talin and ILK, thereby linking the ILK-containing multiprotein adaptor complex to Talin and  $\beta$ PS integrin. Our data suggest that Wech interacts with the head domain of Talin and the kinase domain of ILK. However, we cannot exclude the involvement of other proteins in the physical connection between these core proteins. The *in vitro* and *in vivo* experiments indicate that the Wech BCC and the NHL domains are essential for the functional interaction of Wech with Talin and ILK. In the murine muscles, the single murine Wech orthologue was also strongly colocalized with Talin and ILK. This suggests an evolutionarily conserved role of Wech proteins in the integrin–cytoskeleton link. In addition to Wech, only two other proteins in *Drosophila* contain an NHL domain, the tumour-suppressor proteins Brat<sup>25</sup> and Mei-P26 (ref. 26). The molecular characterization of *brat* mutations suggests that the NHL domain carries the tumour suppressor function of Brat<sup>25</sup>. Whether the tumour suppressor functions of Brat and MeiP-26 involve the modulation of integrin-mediated adhesion through their NHL domains is not known. As a number of clinically relevant disorders are caused by integrin-related adhesive changes, including muscle dystrophies<sup>29</sup>, our finding of a crucial component for integrin adhesive functions may have implications for understanding disease aetiologies.

## METHODS

**Fly strains and rescue experiments.** The following *wech* alleles were used: *P{EP}wech<sup>EP2291</sup>* (Szeged stock FBst0102707), *P{lacW}wech<sup>k08815a</sup>* (Bloomington stock 10818) and *wech<sup>66</sup>*. The *wech<sup>66</sup>* allele is an imprecise excision disrupting the 5' UTR of all three *wech* transcripts and was generated by mobilizing the P-element of *P{EP}wech<sup>EP2291</sup>* (Supplementary Information Methods and Fig. 1). To generate *wech*–GFP transgenic flies, a *wech*–GFP fusion construct was cloned into the pUAST vector (Supplementary Information Methods). Rescue experiments were performed as described in the Supplementary Information Methods using a full-length *wech* cDNA (Genbank accession number BT010087). For mutant analysis

the following fly strains were used: *mys*<sup>XG43</sup> (ref. 30), *rhea*<sup>2</sup> (ref. 14), *integrin-linked kinase-GFP*<sup>13</sup> and *tensin-GFP*<sup>15</sup> (gift from N. Brown, Gurdon Institute, University of Cambridge, UK). Oregon-R flies were used as wild-type controls.

**Immunohistochemistry.** The anti-Wech antibody containing the amino acids 536–550 (LSLSFATEGHEDGQV) was generated in rabbit and affinity-purified by Davids Biotechnology. The antibody was used at a 1:20 dilution for whole-mount antibody staining. Primary antibodies were as follows: anti-DE-cadherin (Santa Cruz Biotechnology), anti-fasciclinIII (1:10, Developmental Studies Hybridoma Bank (DSHB)), anti-even skipped (1:30, DSHB), anti-βPS (1:10, DSHB), anti-αPS2 (1:5), anti-Short Stop (1:1000), anti-Talin (1:20) (gifts from N. Brown), anti-MHC (1:500, gift from D. Kiehart, Durham University, NC), anti-GFP (1:300, Santa Cruz Biotechnology) and anti-PINCH (1:500; gift from M.C. Beckerle, University of Utah). The following secondary antibodies were used: Alexa Fluor 488 (1:200, MoBiTec), Cy3 (1:200, Dianova) and Alexa Fluor 633 (1:100, MoBiTec). For immunofluorescence microscopy of mouse tissues, muscles were isolated from 8-week-old C57Bl/6 mice and stained using KFG2c (rat IgG2c), produced against the peptide 567KFGEGTKNGQFNYPW582 of murine Wech (1:20, Helmholtz Institute), murine anti-Talin C-20 (1:50; Santa Cruz Biotechnology) and murine anti-ILK (1:50; Upstate) antibodies. For further details, see Supplementary Information Methods.

**Western blot analysis.** Primary antibody incubations were performed overnight with 5% (wt/vol) milk powder in Tris-buffered saline containing 0.5% (vol/vol) Tween-20. Anti-flag monoclonal antibody was purchased from Sigma-Aldrich and anti-Myc monoclonal antibody was purchased from Santa Cruz Biotechnology. Incubation with secondary antibodies was performed with peroxidase-coupled goat anti-mouse immunoglobulin (1:15,000, Santa Cruz Biotechnology), followed by enhanced chemiluminescence (Amersham) detection.

Note: Supplementary Information is available on the Nature Cell Biology website.

#### ACKNOWLEDGEMENTS

We would like to thank N. Brown and D. Kiehart for sharing fly stocks and reagents, A. Bill for measuring the intensity of the Wech interactions, D. Fürst for discussion of the murine muscle data, T. Magin, I. Zinke and P. Carrera for comments on the manuscript and the members of the Hoch laboratory for helpful discussions. This work was supported by grants from the Deutsche Forschungsgemeinschaft to M. H. and W. K. (SFB 645).

#### AUTHOR CONTRIBUTIONS

B. L. performed all the *Drosophila* experiments, which were designed together with R. B. and M. H.; W. K. designed the mouse experiments; J. N. characterized the murine Wech 5B7 antibody which was produced by E. K.; R. Bo. performed the sectioning and staining of the murine muscles. All authors discussed the experimental results of the manuscript. M.H. wrote the manuscript.

Published online at <http://www.nature.com/naturecellbiology/>  
Reprints and permissions information is available online at <http://npg.nature.com/reprintsandpermissions/>

- Hynes, R. O. Integrins: bidirectional, allosteric signaling machines. *Cell* **110**, 673–687 (2002).
- Wiesner, S., Legate, K. R. & Fassler R. Integrin-actin interactions. *Cell. Mol. Life Sci.* **62**, 1081–1099 (2005).

- Meroni, G. & Diez-Roux, G. TRIM/RBCC, a novel class of 'single protein RING finger' E3 ubiquitin ligases. *Bioessays* **27**, 1147–1157 (2005).
- Slack, F. J. & Ruvkun, G. A novel repeat domain that is often associated with RING finger and B-box motifs. *Trends Biochem. Sci.* **23**, 474–475 (1998).
- Gumbiner, B. M. Cell adhesion: the molecular basis of tissue architecture and morphogenesis. *Cell* **84**, 345–357 (1996).
- Brown, N. H., Gregory, S. L. & Martin-Bermudo, M. D. Integrins as mediators of morphogenesis in *Drosophila*. *Dev. Biol.* **223**, 1–16 (2000).
- De Arcangelis, A. & Georges-Labouesse, E. Integrin and ECM functions: roles in vertebrate development. *Trends Genet.* **16**, 389–395 (2000).
- Giancotti, F. G. & Ruoslahti, E. Integrin signaling. *Science* **285**, 1028–1032 (1999).
- Hannigan, G., Troussard, A. A. & Dedhar, S. Integrin-linked kinase: a cancer therapeutic target unique among its ILK. *Nature Rev. Cancer* **5**, 51–63 (2005).
- Liu, S., Calderwood, D. A. & Ginsberg, M. H. Integrin cytoplasmic domain-binding proteins. *J. Cell Sci.* **113**, 3563–3571 (2000).
- Wu, C. PINCH, N(1)ck and the ILK: network wiring at cell-matrix adhesions. *Trends Cell Biol.* **15**, 466–466 (2005).
- Brown, N. H. *et al.* Talin is essential for integrin function in *Drosophila*. *Dev. Cell* **3**, 569–579 (2002).
- Zervas, C. G., Gregory, S. L. & Brown, N. H. *Drosophila* integrin-linked kinase is required at sites of integrin adhesion to link the cytoskeleton to the plasma membrane. *J. Cell Biol.* **152**, 1007–1018 (2001).
- Clark, K. A., McGrail, M. & Beckerle, M. C. Analysis of PINCH function in *Drosophila* demonstrates its requirement in integrin-dependent cellular processes. *Development* **130**, 2611–2621 (2003).
- Torgler, C. N. *et al.* Tensin stabilizes integrin adhesive contacts in *Drosophila*. *Dev. Cell* **6**, 357–369 (2004).
- Jiang, G., Giannone, G., Critchley, D. R., Fukumoto, E. & Sheetz, M. P. Two-piconewton slip bond between fibronectin and the cytoskeleton depends on talin. *Nature* **424**, 334–337 (2003).
- Tanentzapf, G. & Brown, N. H. An interaction between integrin and the talin FERM domain mediates integrin activation but not linkage to the cytoskeleton. *Nature Cell Biol.* **8**, 601–606 (2006).
- Giannone, G., Jiang, G., Sutton, D. H., Critchley, D. R. & Sheetz, M. P. Talin1 is critical for force-dependent reinforcement of initial integrin-cytoskeleton bonds but not tyrosine kinase activation. *J. Cell Biol.* **163**, 409–419 (2003).
- Volk, T. Singling out *Drosophila* tendon cells: a dialogue between two distinct cell types. *Trends Genet.* **15**, 448–453 (1999).
- Bokel, C. & Brown, N. H. Integrins in development: moving on, responding to, and sticking to the extracellular matrix. *Dev. Cell* **3**, 311–321 (2002).
- Gregory, S. L. & Brown, N. H. *Kakapo*, a gene required for adhesion between and within cell layers in *Drosophila*, encodes a large cytoskeletal linker protein related to plectin and dystrophin. *J. Cell Biol.* **143**, 1271–1282 (1998).
- Paululat, A., Breuer, S. & Renkawitz-Pohl, R. Determination and development of the larval muscle pattern in *Drosophila melanogaster*. *Cell Tissue Res.* **296**, 151–160 (1999).
- Leptin, M., Bogaert, T., Lehmann, R. & Wilcox, M. The function of PS integrins during *Drosophila* embryogenesis. *Cell* **56**, 401–408 (1989).
- Roote, C. E. & Zusman, S. Functions for PS integrins in tissue adhesion, migration, and shape changes during early embryonic development in *Drosophila*. *Dev. Biol.* **169**, 322–336 (1995).
- Betschinger, J., Mechtler, K. & Knoblich, J. A. Asymmetric segregation of the tumor suppressor *brat* regulates self-renewal in *Drosophila* neural stem cells. *Cell* **124**, 1241–1253 (2006).
- Arama, E., Dickman, D., Kimchie, Z., Shearn, A. & Lev, Z. Mutations in the β-propeller domain of the *Drosophila* brain tumor (*brat*) protein induce neoplasm in the larval brain. *Oncogene* **19**, 3706–3716 (2000).
- Slack, F. J. *et al.* The *lin-41* RBCC gene acts in the *C. elegans* heterochronic pathway between the *let-7* regulatory RNA and the LIN-29 transcription factor. *Mol. Cell* **5**, 659–669 (2000).
- Bendig, G. *et al.* Integrin-linked kinase, a novel component of the cardiac mechanical stretch sensor, controls contractility in the zebrafish heart. *Genes Dev.* **20**, 2361–2372 (2006).
- Mayer, U. Integrins: redundant or important players in skeletal muscles? *J. Biol. Chem.* **278**, 14587–14590 (2003).





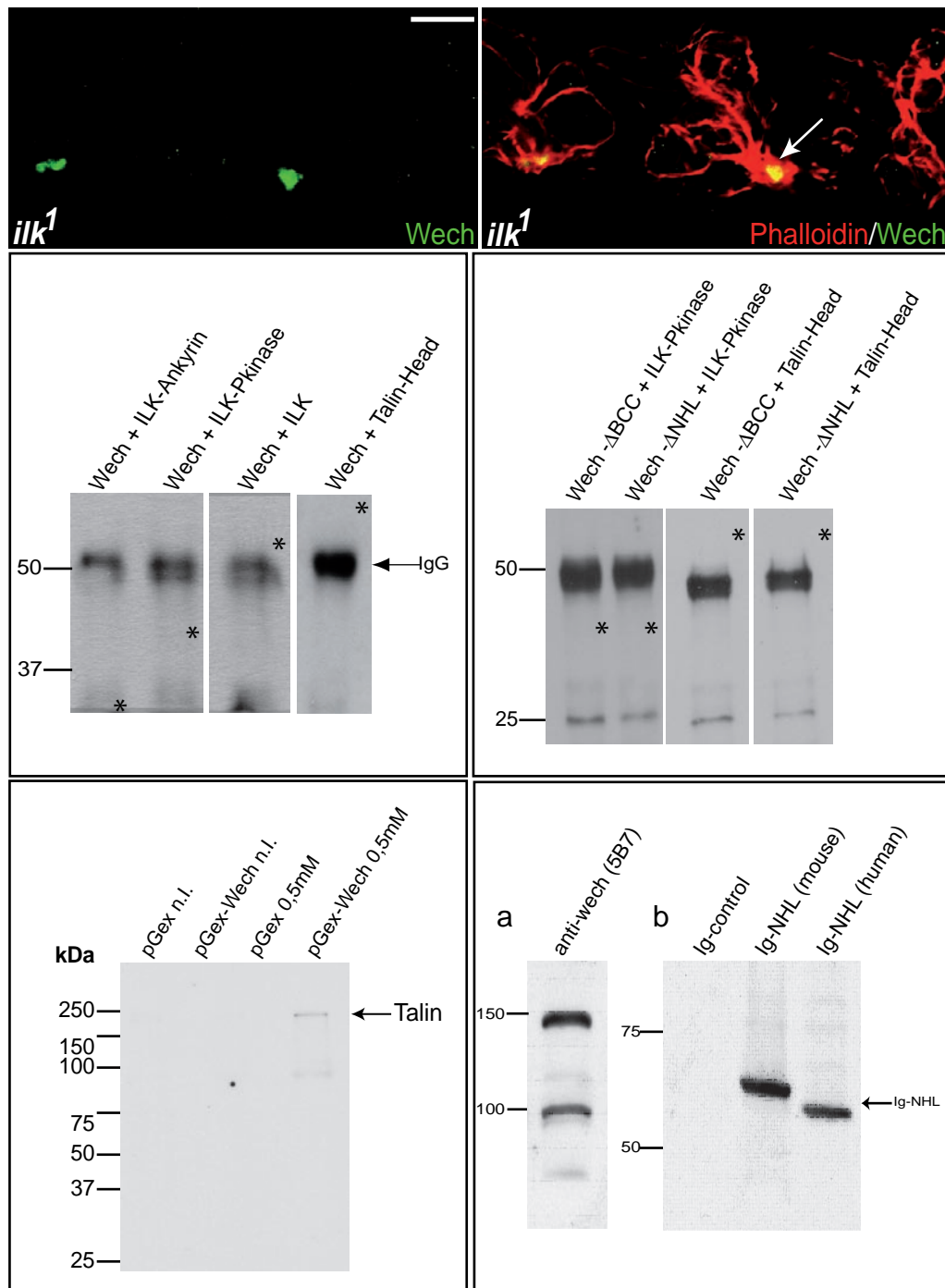


**Figure S3** Wech localization is unaffected in *ilk* mutants, and Wech interacts with Talin *in vivo*. **(a,b)** In *ilk* mutants (stage 16/17), Wech is still expressed in the muscle attachment site (arrow). The rounded up muscles are stained with Phalloidin. **(c,d)** Immunoprecipitation of the different tagged fusion proteins of Wech, ILK and Talin using normal rabbit IgGs as a negative control. No specific signal can be detected in the different reactions (indicated by asterisks). **(e)** GST-pulldown of GST-Wech fusion proteins and the controls using GST alone

(pGex) and induced (0.5mM) and not induced (n.l.) samples. The pulldown was performed with wild type embryo lysate and probed with the anti-Talin antibody. Only the sample with the induced GST-Wech fusion protein shows a specific signal for Talin **(f)** Specificity of anti-Wech mAb 5B7. Endogenous Wech was detected in Jurkat cells by immunoblot, using the anti-Wech antibody 5B7 **(a)**. Immunoprecipitation of Ig-tagged NHL-domain of human and murine Wech. MAb detects the NHL-domain of murine and human Wech **(b)**. Scale bar 10 μm.

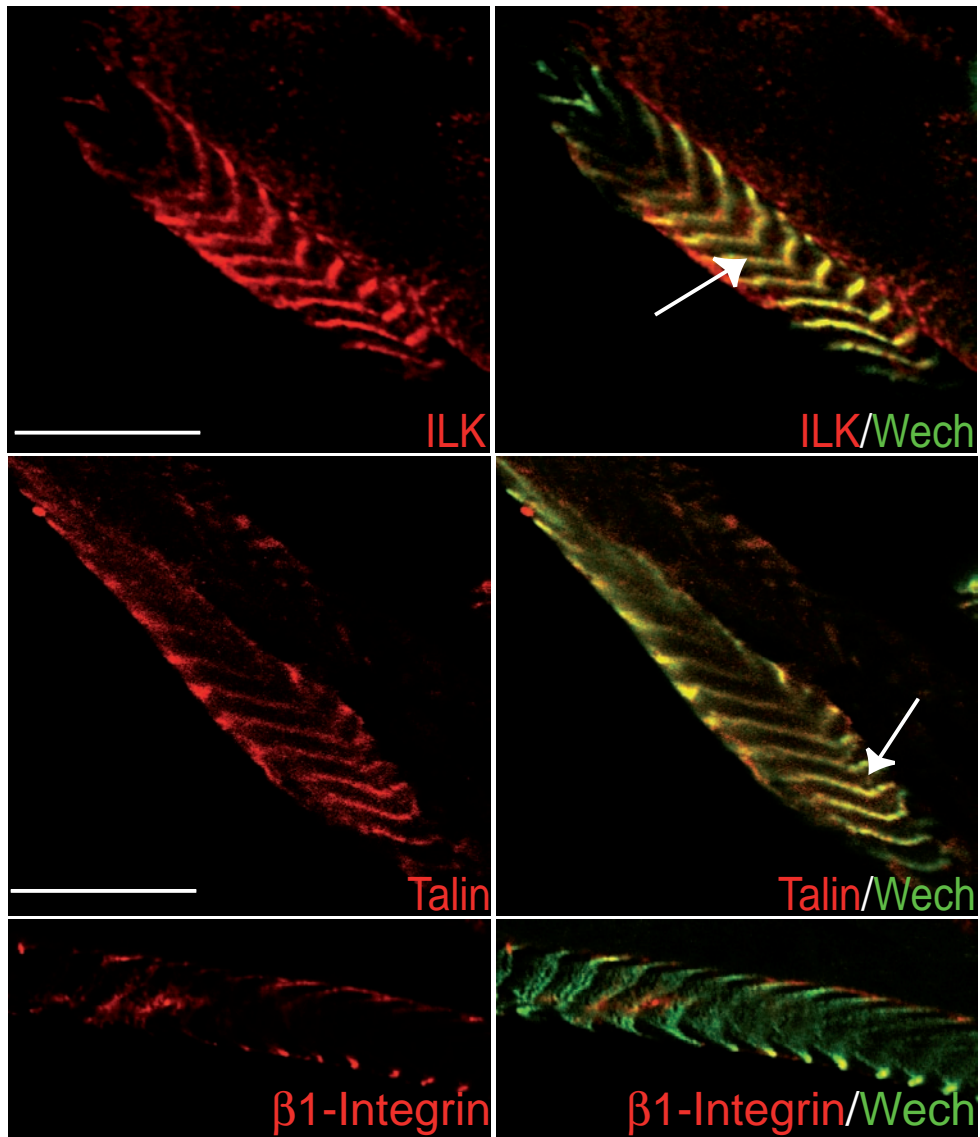


**Figure S4** Murine Wech expression in Z discs of adult mice. a-f, The murine Wech protein is expressed in Z discs of adult mice where it shows

co-localization with ILK (arrow in **b**) and Talin (arrow in **d**), and a partial co-localization with  $\beta$ 1-Integrin at the membrane (**f**). Scale bars 130  $\mu$ m.

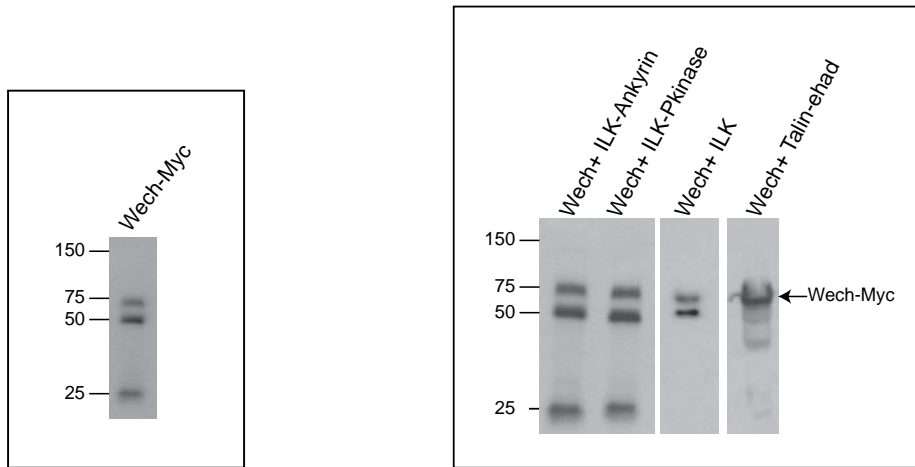


Figure 3c, lower panel

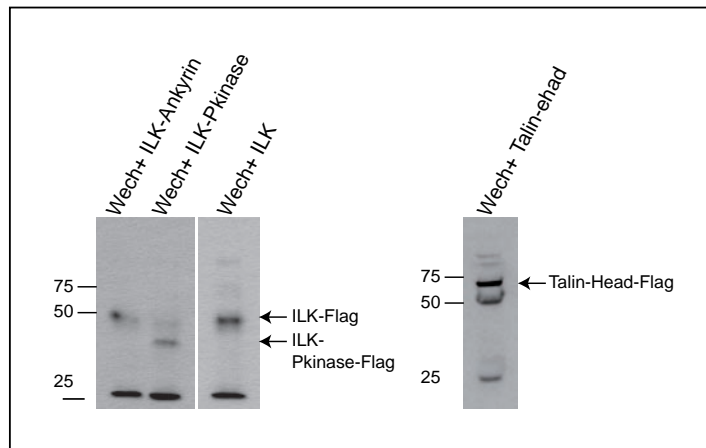


Figure 3e

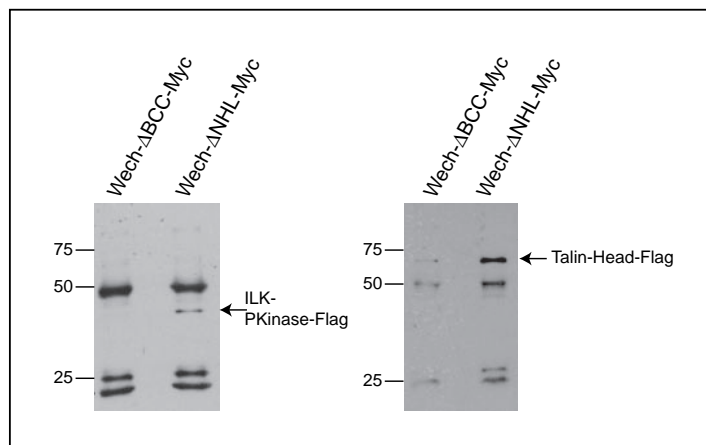


Figure S5 Full scans and panels of key western data.

## Supplementary methods

**Molecular characterization of the *wech* transcripts.** To characterize the three transcripts RA, RB and RC of *wech*, cDNA of Oregon-R wild type flies was prepared according to the “QuantiTect Reverse Transcription” protocol (Qiagen, Hilden, Germany). Primers were as follows:

Pair1:

AGC GCA TGA ACG TGA GTT TTG (*wech* P1)

GCC GTC CTA GGG TAT CCC AT (*wech* P2)

Pair2:

GAG GAA CAG GTA ACG GCA C (*wech* P3)

TTC ACT CTA CGC GTC CTA GG (*wech* P4)

**Fly strains.** The *wech* alleles are  $P\{lacW\}wech^{k08815a}$  (Bloomington stock 10818),  $P\{EP\}wech^{EP2291}$  (Szeged stock FBst0102707) and *wech*<sup>66</sup>. The *wech*<sup>66</sup> allele was generated by mobilizing the P-element in  $P\{EP\}wech^{EP2291}$  with a  $\Delta 2-3$  transposase (see methods section of the main text for further details on the *wech*<sup>66</sup> allele). *wech*<sup>66</sup> was recombined with *FRTG13* (Bloomington stock 1956). To generate germ line clones, these flies were crossed to  $y w hsFLP / Y ; ovo^D FRTG13 / CyO$  males, and the progeny were heat shocked for 2 hr at 37°C. To generate a *wech-GFP* fusion construct, a full length *wech* cDNA (Genbank accession number BT010087) was cloned via *EcoRI/ApaI* sites in frame with the eGFP coding sequence of the pMJ Green vector (gift from K. Willecke). The *wech-GFP* fusion fragment was excised using *EcoRI/NotI* sites and inserted in the pUAST vector to produce *UAS-wech-GFP* transgenic flies. The myc-

tagged deletion constructs of *wech* were amplified by PCR and cloned via *EcoRI/XbaI* in the pCS<sup>+</sup> vector. These fragments were then excised using *EcoRI/XbaI* and inserted in the pUAST vector to produce UAS-Wech-ΔNHL-Myc and UAS-Wech-ΔBCC-Myc transgenic flies. The generation of inducible RNAi fly strains was performed as described by Lee and Carthew (Lee and Carthew, 2003). In general, a 750 bp fragment out of exon four was amplified by PCR and cloned in two different orientations into the pWiz vector (gift of R.W. Carthew). Recombinants with “tail to tail” orientation were selected and used to produce transgenic flies. The nucleotide sequence of all constructs was confirmed by sequencing. In rescue experiments, flies of the genotype *wech*<sup>66</sup> / *CyO* ; *Dmef2-gal4* and *wech*<sup>66</sup> / *CyO* ; *sr-gal4* / *TM3, Sb, Ser* were crossed to *wech*<sup>66</sup> / *CyO* ; UAS-*wech:GFP* males, to express Wech-GFP in a *wech*<sup>66</sup> mutant background. Cell type-specific rescue experiments with *sr-gal4* (tendon cell-specific) or *Dmef2-gal4* (muscle cell-specific) at 29°C rescued the muscle detachment phenotypes of the mutants and the animals survived until 2<sup>nd</sup> instar larval stage, demonstrating a functional requirement of *wech* in both cell types, the tendon and the muscle cell. Additionally rescue experiments were done with flies of the genotype *wech*<sup>66</sup> / *CyO* ; *Dmef2-gal4*; *sr-gal4* / *TM3, Sb, Ser* and *hs-gal4*; *wech*<sup>66</sup> / *CyO* were crossed to *wech*<sup>66</sup> / *CyO* ; UAS-*wech:GFP* males. In these experiments, rescue of the muscle detachment defect could also be obtained when Wech was re-supplied in both the tendon and muscle cells and the rescued animals survived until 3<sup>rd</sup> instar larval stage. For mutant analysis the following fly strains were used: *mys*<sup>XG43</sup>, *rhea*<sup>2</sup>, *integrin-linked kinase-GFP* and *tensin-GFP*, which express the GFP under their endogenous promoters (kind gift of N. Brown). Oregon-R flies were used as wild type control.

**Molecular Biology and Genotype validation.** CG1624 has been previously named *dappled* (*dpld*). However, we have found out that the *dpld* locus does not correspond to CG1624. Therefore we have renamed CG1624 “*wech*”. Genotype verification of P-element mutant flies was performed by PCR. Genomic DNA was prepared according to BDGP “Inverse PCR and cycle sequencing of P-element insertions for STS generation” protocol. Primers were as follows:

P-element insertion *wech*<sup>EP2291</sup>

Pair1:

CAG AAT CAG TGT GAC CAG CC (*wech* F1)

CAC CCA AGG CTC TGC TCC CAC AAT (Plac1)

Pair2:

ACG CCA GCA TGA TTA CTT GT (*wech* F2)

CAC CCA AGG CTC TGC TCC CAC AAT (Plac1)

Pair3:

CTT GCC GAC GGG ACC ACC TTA TGT TAT T (Pry2)

GTA AGC ACA GCG ACG ATA AGC (*wech* R1)

*wech*<sup>66</sup>

Pair1:

CAG AAT CAG TGT GAC CAG CC (*wech* F1)

GTA AGC ACA GCG ACG ATA AGC (*wech* R1)

Pair2:

CAG AAT CAG TGT GAC CAG CC (*wech* F1)

CAC CCA AGG CTC TGC TCC CAC AAT (Plac1)

Pair3:

ACG CCA GCA TGA TTA CTT GT (*wech* F2)

GTA AGC ACA GCG ACG ATA AGC (*wech* R1)

**RNA isolation and *real time* PCR.** *Drosophila* embryos were washed thoroughly with water, transferred to lysis buffer (supplied with RNA isolation kit) and homogenized (Ultra-Turrax T25basic) at full speed for 1 minute. Total RNA was isolated by using the NucleoSpin RNA II kit (Macherey & Nagel, Germany). First strand cDNA reaction was carried out with 500 ng total RNA using the QuantiTect Reverse Transcription Kit (Qiagen, Germany) including DNaseI treatment according to the supplier's protocol. For *real time* PCR the reaction consisted of an aliquot of cDNA (first strand reaction), forward and reverse primers (200 nM final concentration, primer sequences see below) and iQ SYBR Green Supermix (Bio-Rad, Munich, Germany) in a total volume of 25 µl. For each template 3 reactions were done in parallel. These were repeated with independently isolated RNA samples from different egg collections. The experiments were performed with iQ5 *real time* PCR Detection System from Bio-Rad (Munich, Germany). *Ribosomal protein L32* (*RpL32*, *rp49*) was used as reference gene, standard control PCR reactions were carried out to test for contaminations. *Real time* PCR was analysed using BIO-RAD iQ5 Optical System software (version 1.1.1442.OCR), following the instruction provided by the supplier, and Microsoft Excel.

The following oligonucleotides were used for *real time* PCR analysis:

*RpL32*: GCTAAGCTGTGCGACAAATG (*rp49-Real-F1*) GTTCGATCCGTAACCGATGT (*rp49-Real-R1*);

*wech*: TGGTTAAATGCGTGCGTGAA (*wech-Real-For*) CAATCGAACGGCTCCAATTCT(*wech-Real-Rev*).

**Immunohistochemistry.** The peptide LSLSFATEGHEDGQV containing the amino acids 536 to 550 of Wech was synthesized and used to generate an affinity purified anti-Wech rabbit polyclonal antibody. Synthesis and immunization in rabbits was done by Davids Biotechnology (Regensburg, Germany), using standard protocols. The antibody was used at a 1:20 dilution for whole mount antibody staining. Antibody staining was carried out as described earlier<sup>1</sup>. Ethanol-fixation (90% ethanol) was used for all embryonic stainings to allow staining of phalloidin-rhodamin (1:500, Sigma). Primary antibodies were as follows: anti-DE-cadherin (1:50; Santa Cruz Biotechnology, Santa Cruz, CA), anti-fasciclinIII (1:10; Developmental Studies Hybridoma Bank, Iowa City, IA), anti-even skipped (1:30; Developmental Studies Hybridoma Bank, Iowa City, IA), anti- $\beta$ PS (1:10, Developmental Studies Hybridoma Bank, Iowa City, IA), anti- $\alpha$ PS2 (1:5; a gift from N. Brown), anti-Short Stop (1:1000; a gift from N. Brown), anti-MHC (1:500, a gift from D. Kiehart), anti-GFP (1:300; Santa Cruz Biotechnology), anti-Talin (1:20; a gift from N. Brown), and anti-Pinch (1:500; a gift from M.C. Beckerle). The following secondary antibodies were used: Alexa Fluor 488 (1:200; MoBiTec, Goettingen, Germany), Cy3 (1:200, mouse; Dianova, Hamburg, Germany), and Alexa Fluor 633 (1:100; MoBiTec, Goettingen, Germany). Images were collected by confocal microscopy using a Leica TSP2 confocal microscope (Leica, Wetzlar, Germany) and processed using Adobe Photoshop software and assembled using Adobe Illustrator software. For immunostaining of mouse tissues, the following primary antibodies were used: 5B7 against Wech (neat) (GSF, Munich, Germany), Talin C-20 (1:50) (Santa Cruz Biotechnology, Santa Cruz, USA), anti-ILK (1:50) (Upstate, Lake Placid, USA). Secondary antibodies were Alexa 633-conjugated donkey anti-goat (1:200), Cy3-

conjugated goat anti-rabbit (1:200), and FITC-conjugated donkey anti-rat (1:100) (Dianova, Hamburg, Germany).

**Immunofluorescence and analysis of the DA1 muscle.** For analysing the DA1 muscle, whole embryos (stage 16) were stained with the anti-Eve antibody as described above. In total 20 hemi-segments were analysed and the nuclei of each counted. In average, 9 – 10 nuclei were present in each DA1 muscle.

**Immunofluorescence and microscopy of mouse tissues.** For immunofluorescence staining muscles were isolated from 8 weeks old adult C57Bl/6 mice, mounted in Tissue-Tek (Sakura Finetek, NL) and immediately frozen in isopentane at -80°C. A Leica CM1900 cryomicrotome was used to cut sections of 12 µm at -24°C. Frozen sections were air dried on SuperfrostPlus (Merck) glass slides at room temperature for 1 hour and then fixed for 10 minutes at -20°C in acetone and air dried. The sections were encircled with a wax pen (Dako, Hamburg, Germany) and then blocked for 1 hour in 3% BSA in TBS buffer. Sections were incubated for 1 hour in a humidified chamber with 25 µl of the diluted primary antibody in TBS + 1% BSA. The slides were washed three times for 5 minutes with TBS, pH 7.5, before 25 µl of secondary antibody were applied. After 45 minutes of incubation the washing procedure was repeated. The slides were briefly washed with water, ethanol, and air-dried. Coverslips were mounted with Gelmount (Biomed, Foster City, USA) and examined with a confocal microscope (FluoView FV1000, Olympus, Tokyo, Japan). Image analysis and processing were performed using the Olympus FluoView FV1000 (Olympus) and CorelDRAW Graphic Suit 12 software.

**Transfections, co-immunoprecipitation and immunoblotting.**

2 x 10<sup>6</sup> HeLa cells were seeded in a 10mm dish and transfected with pCS<sup>+</sup>-ILK-Ankyrin-Flag, pCS<sup>+</sup>-ILK-Pkinase-Flag, pCS<sup>+</sup>-ILK-Flag, pCS<sup>+</sup>-Talin-Head-Flag, pCS<sup>+</sup>-Wech-ΔBCC-Myc, pCS<sup>+</sup>-Wech-ΔNHL-Myc and pCS<sup>+</sup>-Wech-Myc. Transfection was performed with Metafecten (Biontex, Germany). After 24 hr, cells were harvested and lysed with RIPA-buffer (150 mM NaCl, 1% IGEPAL CA-630, 0.5% sodium deoxycholate, 0.1% SDS, 50 mM Tris [pH 8.0] supplemented with protease-inhibitor-mix (complete, Roche, Mannheim). cDNA of Ig-tagged NHL-domain of human or murine *wech* was transfected by electroporation. 1 x 10<sup>7</sup> cells from exponentially grown cultures were electroporated at 240 V and 1500 μF with 20 μg of DNA, using a Bio-Rad Gene Pulser (Bio-Rad, Munich, Germany). 24 h after transfection, cells were lysed in Igepal lysis buffer (10 mM HEPES [pH 7.5], 10 mM KCl, 10 mM MgCl<sub>2</sub>, 150 mM NaCl, 1% Igepal and supplemented with protease-inhibitors Aprotinin, Leupeptin, and PMSF).

To analyse the expression of endogenous Wech in Jurkat cells, Jurkat E6 cells were lysed in Igepal lysis buffer (10 mM HEPES [pH 7.5], 10 mM KCl, 10 mM MgCl<sub>2</sub>, 150 mM NaCl, 1% Igepal, supplemented with protease-inhibitors Aprotinin, Leupeptin and PMSF). Cell lysates (10 μg of protein) were separated by SDS-PAGE and transferred onto nitrocellulose. Endogenous Wech was detected using the anti-Wech antibody 5B7 (1:20). Co-immunoprecipitation was performed using the immunoprecipitation starter pack (Amersham Biosciences, Piscataway, NJ) according to the manufacturer's instruction. To avoid nonspecific binding of proteins to A/G-Sepharose, preclearing of the cell-lysate was performed in the presence of protein A/G-Sepharose according to the

manufacturer's manual. Accordingly, antibody incubation and precipitation of the immune complexes from the precleared lysate was done in RIPA-buffer (Igepal-buffer) in a final volume of 500  $\mu$ l. The immunoprecipitation samples were incubated for 1 h at 4°C with mouse monoclonal anti-c-Myc antibody 9E10 (c-Myc 9E10; Santa Cruz Biotechnology). As a control, we used normal mouse-IgG (Santa Cruz Biotechnology, Santa Cruz, CA). Protein A/G-Sepharose (Amersham Biosciences) was added at a final volume of 40 $\mu$ l to each mixture and incubated for 2 h at 4°C. Afterwards, beads were washed 3 times with RIPA-buffer (Igepal-buffer) and 3 times with ice cold PBS. Immunoblots were blocked using Tris-buffered saline plus 0.05% Tween with nonfat dry milk. Washes were performed in Tris-buffered saline plus 0.05% Tween without milk. Bound antigen was detected by enhanced chemiluminescence (Amersham Biosciences). The antibodies for immunoblotting were diluted in Tris-buffered saline plus 0.05% Tween and used at the following concentrations: anti-Flag M2 (1:2000, Sigma-Aldrich), anti- c-Myc 9E10 (1:500; Santa Cruz Biotechnology, Santa Cruz, CA), anti Wech mAB 5B7 (neat), and anti-mouse-HRP (1:15000; Santa Cruz Biotechnology, Santa Cruz, CA).

The measurement of the protein interactions between Talin-head and the Wech deletion constructs was performed using a VersaDoc 5000 (BioRad, Munich, Germany) and analysed using the Quantity One 4.6.1 software (BioRad, Munich, Germany).

### **GST purification and pulldown with embryonic lysate.**

For GST purification of the complete Wech protein, the *wech* open reading frame was subcloned in frame with GST in the pGEX-5x vector from Stratagene. The fusion protein was expressed in *E. coli* cells using the BL21 strain from Stratagene. Cells were

grown on 37°C, induced at OD<sub>600</sub> of 0.8 with 0.25 mM IPTG and incubation was continued at 25°C for 4 hours. Afterwards, the cells were harvested in lysis buffer (1x PBS; 0.5% Tween; 0,2 mg/ml lysozyme and supplemented with protease-inhibitors) and incubated overnight with 500µl glutathione sepharose beads (Amersham Biosciences). The beads were washed 10 times with ice cold lysis buffer and 50µl each were then incubated for 4 hours with the appropriate embryo lysate (wild type or ILK-GFP). Western-blotting and detection was performed as described above.

1. Bauer, R., Lehmann, C., Martini, J., Eckardt, F., and Hoch, M. Gap junction channel protein innexin 2 is essential for epithelial morphogenesis in the *Drosophila* embryo. *Mol Biol Cell* **15**, 2992-3004 (2004).
2. Lee Y.S. and Carthew R.W. Making a better RNAi vector for *Drosophila*: use of intrin spacers. *Methods* **30 (4)**, 322-329 (2003).